Atmospheric CO_2 concentrations during ancient greenhouse climates were similar to those predicted for A.D. 2100

D. O. Breecker[1,2], Z. D. Sharp, and L. D. McFadden

MSC03-2040, Department of Earth and Planetary Sciences, University of New Mexico, Albuquerque, NM 87131

Edited by Thure E. Cerling, University of Utah, Salt Lake City, UT, and approved October 22, 2009 (received for review March 5, 2009)

Quantifying atmospheric CO_2 concentrations ($[CO_2]_{atm}$) during Earth's ancient greenhouse episodes is essential for accurately predicting the response of future climate to elevated CO_2 levels. Empirical estimates of $[CO_2]_{atm}$ during Paleozoic and Mesozoic greenhouse climates are based primarily on the carbon isotope composition of calcium carbonate in fossil soils. We report that greenhouse $[CO_2]_{atm}$ have been significantly overestimated because previously assumed soil CO_2 concentrations during carbonate formation are too high. More accurate $[CO_2]_{atm}$, resulting from better constraints on soil CO_2, indicate that large (1,000s of ppmV) fluctuations in $[CO_2]_{atm}$ did not characterize ancient climates and that past greenhouse climates were accompanied by concentrations similar to those projected for A.D. 2100.

paleosol barometer | carbon isotopes | pedogenic carbonate | Phanerozoic | climate sensitivity

The anthropogenically driven rise in $[CO_2]_{atm}$ is well established (1) but its effect on future climate is less certain (2). Many recent studies indicate that $[CO_2]_{atm}$ has controlled or strongly amplified Phanerozoic (542 Ma–present) climate variations (3–8) and therefore understanding the relationship between $[CO_2]_{atm}$ and climate over geologic time provides crucial empirical constraints on the magnitude of future global warming (1, 9). Estimates of Paleozoic and Mesozoic $[CO_2]_{atm}$ are largely based on the soil carbonate CO_2 paleobarometer (10), which is the most temporally continuous proxy (indicator) for $[CO_2]_{atm}$ over the past 400 million years. The CO_2 paleobarometer is also considered the most reliable provider of $[CO_2]_{atm}$ estimates for times when $[CO_2]_{atm}$ was significantly above modern values (11). The CO_2 paleobarometer suggests that $[CO_2]_{atm}$ values exceeded 3,000 parts per million by volume (ppmV) during Permian (289–251 Ma) and Mesozoic (251–65 Ma) greenhouse climates (5, 8, 12). However, other $[CO_2]_{atm}$ proxies, which are either considered to be less reliable at high $[CO_2]_{atm}$ (stomatal index) or are newly developed and therefore less widely utilized (e.g., fossil bryophytes), typically result in $[CO_2]_{atm}$ estimates for greenhouse climates that are much lower than estimates from soil carbonate (5, 6). The large discrepancy among proxies can be interpreted two ways: 1) large (1,000s of ppmV) variations in $[CO_2]_{atm}$ occurred over relatively short time periods (in certain cases shorter than the temporal resolution of the proxy records) throughout the Phanerozoic or 2) some of the proxy estimates are inaccurate. In this study we use data from modern soils and incorporate an improved understanding of pedogenic carbonate formation to recalibrate the CO_2 paleobarometer. We report that the most often quoted $[CO_2]_{atm}$ values, those previously determined from pedogenic carbonate, are too high, and that paleo $[CO_2]_{atm}$ values did not persist above 1,500 ppmV during the past 400 million years.

Pedogenic (soil) carbonate (calcite, $CaCO_3$) forms in soils where potential evapotranspiration exceeds precipitation, typically in arid to subhumid regions that receive less than 100 cm of rain per year. $Ca^{2+}_{(aq)}$, released primarily by the dissolution of Ca-bearing minerals in dust (13) is carried to depth by downward-percolating water and eventually reprecipitates as pedogenic carbonate. The dissolution and precipitation of calcite in soils occurs by the reaction:

$$Ca^{2+} + 2HCO_3^- \leftrightarrow CaCO_3 + H_2O + CO_2$$

and the following equation illustrates changes in the soil environment that can drive calcite precipitation

$$a_{CaCO_3} = \frac{4m^3_{Ca^{2+}}}{pCO_2}\left(\frac{K_2}{K_1 K_{cal} K_{CO_2}}\right) \quad [1]$$

where a_{CaCO_3} is the activity of calcite; $m_{Ca^{2+}}$ is the concentration of calcium ions in aqueous solution; pCO_2 is the partial pressure of CO_2 in the soil gas; and K_1, K_2, K_{cal}, and K_{CO_2} are temperature-sensitive equilibrium constants for the dissociation of carbonic acid, the dissociation of bicarbonate, the dissociation of calcite, and the hydration of CO_2, respectively. Eq. **1** is valid for the system $CaCO_3$-H_2O-CO_2 assuming activities equal concentrations and pH < 9. At thermodynamic equilibrium, calcite will precipitate when a_{CaCO_3} reaches a value of 1. The value of a_{CaCO_3} is increased by the following changes: 1) an increase in the concentration of Ca^{2+} in soil solution, 2) a decrease in soil pCO_2, or 3) an increase in soil temperature (the product of the equilibrium constants increases with temperature, meaning calcite is less soluble at higher temperature). Quantification of $m_{Ca^{2+}}$ required for a_{CaCO_3} to reach a value of 1 under seasonally varying soil conditions indicates that the simultaneous occurrence of evapotranspiration, degassing of CO_2, and heating of the soil probably drives pedogenic carbonate formation (14).

Pedogenic carbonate is thought to form in carbon isotope ($^{13}C/^{12}C$) equilibrium with soil CO_2 (CO_2 in the gas-filled soil pore spaces) because carbonate precipitates slowly and changes in the soil environment below 20–30 cm occur relatively slowly. Therefore, pedogenic carbonates provide a record of the carbon isotope composition of coexisting soil CO_2. The carbon isotope composition of soil CO_2 is, in turn, influenced by $[CO_2]_{atm}$ because CO_2 in soil pore spaces is a mixture between atmospheric CO_2 and CO_2 respired by organisms in the soil (15). Thus, measured carbon isotope compositions of pedogenic carbonate can be used to calculate $[CO_2]_{atm}$ at the time the carbonate formed using the following equation derived from an isotope mass balance relationship (16):

$$[CO_2]_{atm} = S(z)\frac{\delta^{13}C_s - 1.0044\delta^{13}C_r - 4.4}{\delta^{13}C_a - \delta^{13}C_s} \quad [2]$$

Author contributions: D.O.B., Z.D.S., and L.D.M. designed research; D.O.B. performed research; D.O.B. and Z.D.S. analyzed data; and D.O.B. wrote the paper.

The authors declare no conflict of interest.

This article is a PNAS Direct Submission.

See Commentary on page 517.

[2]To whom correspondence should be addressed. E-mail: breecker@jsg.utexas.edu.

[1]Present address: Department of Geological Sciences, University of Texas, Austin, TX 78712

Table 1. Compilation of soil surface CO_2 fluxes.

Ecosystem	Soil Order	max J_o*	min† J_o	max $S(z)$ (ppmV)	min $S(z)$ (ppmV)	Ref.
temperate grassland	Vertisol	55.5	3.5	25,700	1,620	(19)
temperate grassland	Mollisol	26.1	6.3	12,100	2,920	(20)
temperate grassland	Mollisol	57.6	3.6	26,700	1,670	(21)
temperate grassland	Mollisol	20.0	4.2	9,300	1,940	(22)
temperate grassland	Inceptisol slightly calcareous	28.8	3.6	13,300	1,670	(23)
tropical grassland	alluvial soil	29.2	4.6	13,500	2,130	(24)
tropical grassland	Oxisol	13.5	6.5	6,200	3,010	(25)
tropical forest	Oxisol	3.5	1.7	3,200	1,560	(26)
tropical forest	Oxisol	11.0	1.5	10,100	1,380	(27)

*J_o is the soil surface CO_2 flux in mmol/m^2/hr

†Minimum summer values are shown for the temperate grasslands; minimum annual values are shown for tropical soils

where $S(z)$ is the soil-derived component of total CO_2 in the soil (i.e., $S(z) = [CO_2]_{soil} - [CO_2]_{atm}$) at depth z; $\delta^{13}C$ is the carbon isotope composition in standard delta notation;* s, r, and a refer to soil CO_2, soil-derived (respired) CO_2, and atmospheric CO_2, respectively; and the coefficient 1.0044 and the constant 4.4 derive from the difference in diffusivity between $^{13}CO_2$ and $^{12}CO_2$.

In order to determine ancient $[CO_2]_{atm}$, the value of $\delta^{13}C_s$ used in Eq. **2** is calculated from measured $\delta^{13}C$ values of carbonate preserved in paleosols (fossil soils) using the temperature-dependent carbon isotope fractionation factor between CO_2 and calcite (17). Values for carbonate formation temperature, $\delta^{13}C_a$, and $\delta^{13}C_r$ are either assumed or estimated from other proxies.† Values for $S(z)$ were originally and somewhat arbitrarily assumed to be ~5,000–10,000 ppmV (10). That range was primarily based on mean growing season CO_2 concentrations in modern soils that do not contain pedogenic carbonate (16, 18) and with only a few exceptions (e.g., 8) has yet to be substantially revised. Efforts to determine the range for $S(z)$ through measurement of soil CO_2 concentrations in modern calcic soils are notably lacking. Therefore, values for $S(z)$ that are appropriate in Eq. **2** remain poorly constrained despite the fact that calculated values of $[CO_2]_{atm}$ are directly proportional to $S(z)$. Improved estimates of $S(z)$ are required to increase the accuracy and reduce the uncertainty in estimates of paleoatmospheric CO_2 concentrations.

Results

We have determined that pedogenic carbonate does not form under mean growing season soil conditions (14) as had previously been assumed (10, 12, 16) and therefore appropriate values for $S(z)$ are significantly less than 5000 ppmV. Results from monitoring the concentration and stable isotope composition of soil CO_2 in central New Mexico demonstrate that pedogenic carbonate forms under seasonally warm and very dry conditions (14). As a soil warms and dries, all of the variables in Eq. **1** change in such as way as to contribute to an increase in a_{CaCO_3}: temperature increases, $m_{Ca^{2+}}$ increases as water is removed from the soil, and soil pCO_2 decreases as soil respiration rates become moisture limited. The observation that low soil CO_2 concentrations help drive the precipitation of calcite in soils suggests that the value of $S(z)$ during pedogenic carbonate formation is significantly lower than it is during mean growing season conditions. $S(z)$ during pedogenic carbonate formation is below 1,000 ppmV in the desert soils studied and is below 2,500 ppmV in soils forming in a Piñon-Juniper Woodland despite the fact that CO_2 concentrations in these soils increase to values of ~3,000 and ~7,000 ppmV, respectively, during the wet summer monsoon season (14). The lower values attending carbonate formation are valid for soils forming in semiarid regions and are the only published values of $S(z)$ during pedogenic carbonate formation (14).

Clay-rich paleosols that formed in moister (subhumid) regions with temperate and tropical climates are commonly used for paleoatmospheric CO_2 barometry. A compilation of minimum CO_2 flux measurements from calcic, clay-rich soils in temperate grasslands, tropical grasslands, and tropical forests suggest that $S(z)$ values in these soils decrease below 2,500 ppmV during dry, hot episodes (Table 1). Therefore, despite the fact that mean annual soil CO_2 concentrations in temperate and tropical soils are generally higher than in desert soils, the $S(z)$ values that occur in clay-rich soils from subhumid regions are similar to those that occur in gravelly soils from semarid regions during hot, dry episodes when pedogenic carbonate forms. A compilation of soil CO_2 concentration measurements supports the idea that large seasonal variations in soil CO_2 concentration occur in calcic soils and that warm-season $S(z)$ values can decrease below 2,500 ppmV, even in climates with mean annual precipitation in excess of half a meter per year (28–31, Fig. 1).

The large variations in soil CO_2 concentrations indicated in Table 1 and Fig. 1 may be the most important factor influencing pedogenic carbonate formation and are probably a universal characteristic of calcic soils. The high CO_2 concentrations during

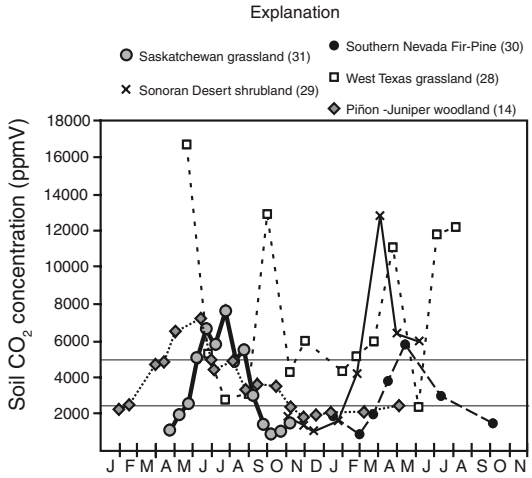

Fig. 1. A compilation of observed seasonal variations in soil pore space CO_2 concentrations. Data from modern calcic soils with native vegetation are shown. The soil atmosphere was sampled from soil gas wells installed below 50 cm in all studies. Mean annual precipitation (cm) for each study site is: New Mexico Piñon-Juniper woodland = 38, West Texas grassland = 40, Sonoran Desert shrubland = 30, Southern Nevada Fir-Pine = 55, Saskatchewan grassland = 35. Thin, horizontal lines highlight 5,000 ppmV, typically used for paleosol barometry, and 2,500 ppmV, a more accurate estimate of $S(z)$ during pedogenic carbonate formation in most soils.

*$\delta^{13}C = (\frac{R_{sam}}{R_{std}} - 1)1000$, where R equals $^{13}C/^{12}C$ and the subscripts "sam" and "std" refer to the unknown sample and a standard (Pee Dee Belemnite, PDB), respectively.

†Soil temperature (needed to calculate $\delta^{13}C_s$) is typically assumed; $\delta^{13}C_a$ is either held constant (10) or is estimated from the $\delta^{13}C$ value of contemporaneous marine carbonates (e.g., 12) or well-preserved organic material (e.g., 8); $\delta^{13}C_r$ is either calculated from $\delta^{13}C_a$ (e.g. 12) or taken to equal the $\delta^{13}C$ value of well-preserved organic material (e.g. 8).

warm, wet periods of the year are responsible for carbonate dissolution and the mobilization of Ca^{2+}, whereas decreasing concentrations associated with hot, dry periods are responsible for carbonate precipitation. Therefore, appropriate values for $S(z)$ in Eq. **2** are not those that occur during mean growing season conditions when $[CO_2]_{soil}$ is near its highest, but rather those that occur during hot, dry periods when $[CO_2]_{soil}$ is near its lowest value and pedogenic carbonate is forming.

A calibration of the CO_2 paleobarometer using Holocene (11.7 ka–present) pedogenic carbonate supports the idea that $S(z)$ values during carbonate formation in soils are lower than previously thought. Table 2 shows values of $S(z)$ that were calculated by solving Eq. **2** for $S(z)$ and then evaluating the resulting expression using measured values of all of the other variables. Previously compiled $\delta^{13}C$ values of pedogenic carbonate from Holocene soils in different climates (12) were used with soil temperatures 5 °C higher than the mean growing season soil temperatures reported by (12) (characteristic of hot, dry periods) (14) to calculate $\delta^{13}C_s$. $[CO_2]_{atm}$ and $\delta^{13}C_a$ were set to their preindustrial values of 280 ppmV and −6.5‰, respectively (32). $\delta^{13}C_r$ values were taken as the $\delta^{13}C$ values of organic matter in the soils, which were reported previously (12). The resulting mean $S(z)$ value is 2,800 ppmV, approximately half the typically assumed value of 5,000 ppmV and similar to $S(z)$ values determined from surface efflux measurements and the stable isotope-based study of soil carbonate formation (14). The calculated $S(z)$ values in Table 2 range from 1,000 to 6,000 ppmV, suggesting that the uncertainty in $S(z)$ for any one soil is currently quite large. Calculating $S(z)$ from measurements of the depth to the soil carbonate horizon (33) may eventually reduce uncertainty in $S(z)$. However, this technique would benefit from the consideration of all of the factors that influence the depth of carbonate in soils (34) and a calibration in which the $S(z)$ values during carbonate formation are determined and the depth to carbonate is measured in the same soils.

Discussion

Atmospheric CO_2 concentrations through the past 400 million years were recalculated in this study using an $S(z)$ value of 2,500 ppmV, which is our best estimate for $S(z)$ based on the results

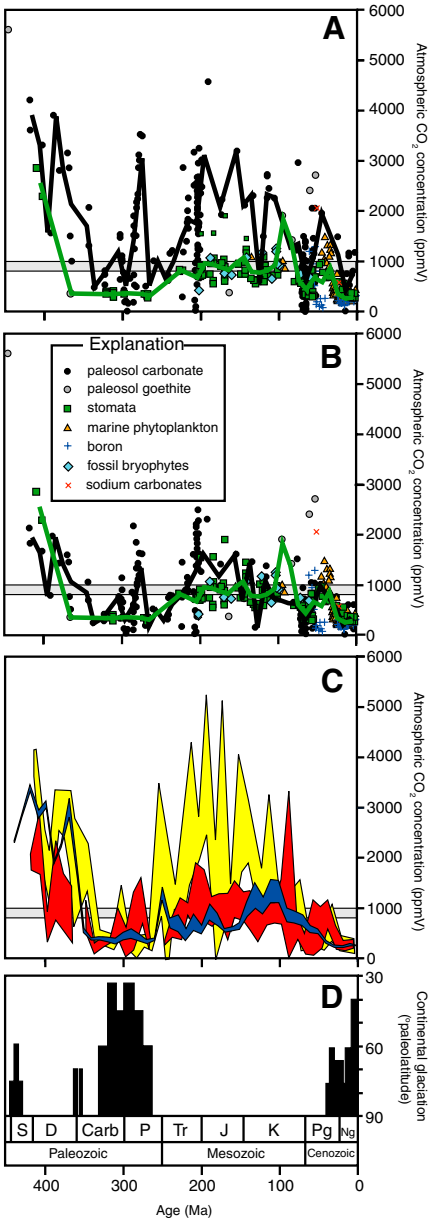

Fig. 2. A compilation of Phanerozoic atmospheric CO_2 records. (*A*) A compilation of atmospheric CO_2 records from different proxies. Paleosol carbonate-based estimates are from original papers in which $S(z)$ values between 4,000 and 10,000 ppmV were used in Eq. **2**. Compilation from (5) with additional proxy-based CO_2 estimates (6, 8, 37, 39–48, D. Royer, pers. comm.). 10 million year bin means of the paleosol carbonate-based estimates and of all the other proxy-based estimates are shown by the black and green lines, respectively. (*B*) Same as Fig. 2*A* with $[CO_2]_{atm}$ estimates from paleosol carbonate recalculated using $S(z) = 2500$ ppmV (see *Methods*). The estimates from paleosol carbonate (black curve) and all other proxies (green curve) are in far better agreement than they are in Fig. 2*A* (two goethite data points at 6,300 ppmV (174 and 188 Ma) were not included in the 10 million year bin means shown in Fig. 2*A* and Fig. 2*B* because these outliers have a strong influence on the averages and may represent transient fluctuations rather than typical Mesozoic atmospheric conditions). (*C*) Comparison of the $[CO_2]_{atm}$ estimates from proxies with $[CO_2]_{atm}$ estimates from GEOCARBSULF (38). The region shown for GEOCARBSULF output (the blue region in front) incorporates the full range of temporal variability in granite $^{87}Sr/^{86}Sr$ values considered in the model. The most recently published compilation of proxy-based $[CO_2]_{atm}$ estimates (9) is shown in yellow (10 million year bins means $\pm 1\sigma$). The revised proxy-based estimates (10 million year bin means $\pm 1\sigma$ shown in red) are generally in good agreement with the GEOCARBSULF model results and are substantially lower than the most recent compilation of proxy-based estimates. (*D*) Paleolatitudinal extent of Phanerozoic glaciations (49) showing the strong correlation between $[CO_2]_{atm}$ and glaciation. CO_2 concentrations predicted for the year A.D. 2100, assuming a heterogeneous world in which technological advancements spread slowly, population grows continuously, and economic development is primarily regional rather than global (2) (SRES anthropogenic emissions scenario A2), are shown as the horizontal gray bar in *A*, *B*, and *C*. Figure modified from (5).

Table 2. Values of $S(z)$ calculated from Holocene soils.

	$\delta^{13}C_r$*	$\delta^{13}C_a$*	$\delta^{13}C_{p.c.}$*	Soil T (°C)†	$\delta^{13}C_s$	atm CO_2 (ppmV)	$S(z)$ (ppmV)
Bolivia	−23.3	−6.5	−8.5	16	−18.4	280	5,300
France	−25.0	−6.5	−10.0	17	−19.7	280	3,838
Greece	−25.7	−6.5	−9.3	19	−18.8	280	1,329
Greece	−23.7	−6.5	−7.5	19	−17.0	280	1,245
Nevada	−23.7	−6.5	−8.5	12	−18.8	280	6,139
Nevada	−23.9	−6.5	−8.5	11	−19.0	280	5,389
Nevada	−23.4	−6.5	−6.8	13	−17.0	280	1,433
New York	−25.6	−6.5	−9.4	21	−18.7	280	1,297
Saskatchewan	−24.2	−6.5	−7.9	20	−17.3	280	1,168
Saskatchewan	−24.1	−6.5	−8.4	20	−17.8	280	1,586
Turkey	−24.5	−6.5	−10.0	23	−19.0	280	3,019
Turkey	−24.5	−6.5	−10.3	23	−19.3	280	4,151
Utah	−24.5	−6.5	−7.4	16	−17.3	280	1,034
Utah	−24.4	−6.5	−7.5	16	−17.4	280	1,120
Utah	−23.8	−6.5	−8.8	16	−18.7	280	4,094
mean							2,809
1σ							1,842

*$\delta^{13}C$ values are reported in ‰ vs PDB
†5 °C higher than temperature used by Ekart et al 1999.

discussed above. The recalculated $[CO_2]_{atm}$ values are compared with previously published CO_2 records in Fig. 2. The recalculated values are up to 2,500 ppmV lower than those previously estimated from pedogenic carbonate (5, 12) and fall into agreement with estimates from other proxies (e.g., 6, 35–37) (Fig. 2*B*), thereby reconciling much of the discrepancy that had existed among different proxies. The recalculated proxy-based $[CO_2]_{atm}$ values are also in good agreement with $[CO_2]_{atm}$ values from the most recent version of the GEOCARB carbon cycle model (38) (Fig. 2*C*). The use of a single $S(z)$ value for all paleosols is certainly a simplification and is being refined currently by further study of modern soils. However, $S(z) = 2,500$ ppmV is appropriate for averages of large numbers of paleosols, and we argue that it improves $[CO_2]_{atm}$ estimates for much of the Phanerozoic.

Until now, the apparent disagreement among proxy estimates has obscured our understanding of paleo $[CO_2]_{atm}$. Reconciling the discrepancy between CO_2 estimates from paleosol carbonate and other techniques indicates that large (1,000s of ppmV) variations in $[CO_2]_{atm}$ did not characterize the Mesozoic Era. Moreover, the agreement between multiple proxies strongly supports the conclusion that the warmest episodes of the Mesozoic were associated with $[CO_2]_{atm}$ equal to $\sim 1,000$ ppmV rather than 2,000–3,000 ppmV (5, 8) (compare Fig. 2*A* and *B*). The relatively low $[CO_2]_{atm}$ of 1,000 ppmV during greenhouse episodes suggest that either Mesozoic warmth was partially caused by a factor unrelated to CO_2 or that the Earth's climate is much more sensitive to atmospheric CO_2 than previously thought.

Comparison of projected future $[CO_2]_{atm}$ (2) with results from the recalibrated CO_2 paleobarometer (Fig. 2*B*) indicate atmospheric CO_2 may reach levels similar to those prevailing during the vegetated Earth's hottest greenhouse episodes by A.D. 2100. The abrupt increase in $[CO_2]_{atm}$ during the Early Permian is similar in magnitude to that possible for the next century in the absence of CO_2 mitigation (Fig. 2*B*). Given that the Early Permian CO_2 increase may have caused the termination of the Late Paleozoic Ice Age (7, 8, Fig. 2*D*), the only known icehouse-greenhouse transition on a vegetated Earth, the effects that unmitigated CO_2 increases may have on future climate warrant careful consideration.

Materials and Methods

Individual $[CO_2]_{atm}$ estimates based on paleosol carbonate were recalculated in this study using:

$$[CO_2]_{atm,recalc} = [CO_2]_{atm,old}\left(\frac{S(z)_{new}}{S(z)_{old}}\right)$$

where $[CO_2]_{atm,old}$ is the previously reported value, $S(z)_{old}$ is the $S(z)$ value originally used to calculate $[CO_2]_{atm,old}$ (4,000–10,000 ppmV), and $S(z)_{new}$ is equal to 2,500 ppmV. $S(z)$ values in modern clay-rich soils were calculated from soil surface CO_2 flux measurements using a steady state production-diffusion model (16). The average depth of soil respiration used in the model was 10 cm for grassland ecosystems and 20 cm for forest ecosystems. Soil porosity, tortuosity, and temperature were assumed to be 0.4, 0.6, and 25 °C, respectively.

ACKNOWLEDGMENTS. We thank J. Quade, L.D. Barnes, S.W. Breecker, F.M. Phillips, and J.R. O'Neil for comments and discussion. We also thank D. Royer and N. Tabor for insightful reviews that substantially improved this paper. D. Royer provided a compilation of proxy-based CO_2 estimates. Financial support was provided by the Caswell Silver Foundation to D.O.B. and by the National Science Foundation EAR 0642822 to Z.D.S. and L.D.M.

1. Jansen E, et al. (2007) *Climate Change 2007: The Physical Science Basis. Contribution of Working Group I to the Fourth Assessment Report of the Intergovernmental Panel on Climate Change*, eds Solomon S, et al. (Cambridge Univ Press, Cambridge), pp 433–497.
2. Meehl GA, et al. (2007) *Climate Change 2007: The Physcial Science Basis. Contribution of Working Group I to the Fourth Assessment Report of the Intergovernmental Panel on Climate Change*, eds Solomon S, et al. (Cambridge Univ Press, Cambridge), pp 747–845.
3. Came RE, et al. (2007) Coupling of surface temperature and atmospheric CO_2 concentrations during the Palaeozoic era. *Nature*, 449:198–201.
4. Royer DL, Berner RA, Montañez IP, Tabor NJ, Beerling DJ (2004) CO_2 as a primary driver of Phanerozoic climate. *GSA Today*, 14:4–10.
5. Royer DL (2006) CO_2-forced climate thresholds during the Phanerozoic. *Geochim Cosmochim Acta*, 70:5665–5675.
6. Fletcher BJ, Brentnall SJ, Anderson CW, Berner RA, Beerling DJ (2008) Atmopsheric carbon dioxide linked with Mesozoic and early Cenozoic climate change. *Nat Geosci*, 1:43–47.
7. Horton DE, Poulsen CJ, Pollard D (2007) Orbital and CO_2 forcing of late Paleozoic continental ice sheets. *Geophys Res Lett*, 34:L19708–L19713 doi:10.1029/2007GL031188.
8. Montañez IP, et al. (2007) CO_2-forced climate and vegetation instability during late Paleozoic deglaciation. *Science*, 315:87–91.
9. Royer DL, Berner RA, Park J (2007) Climate sensitivity constrained by CO_2 concentrations over the past 420 million years. *Nature*, 446:530–532.
10. Cerling TE (1991) Carbon dioxide in the atmosphere: Evidence from Cenozoic and Mesozoic paleosols. *Am J Sci*, 291:377–400.
11. Royer DL, Berner RA, Beerling DJ (2001) Phanerozoic atmospheric CO_2 change: Evaluating geochemical and paleobiological approaches. *Earth-Sci Rev*, 54:349–392.
12. Ekart DD, Cerling TE, Montañez IP, Tabor NJ (1999) A 400 million year carbon isotope record of pedogenic carbonate: Implications for paleoatmospheric carbon dioxide. *Am J Sci*, 299:805–827.
13. Birkeland PW (1999) *Soils and Geomorphology* (Oxford Univ Press, Oxford) p 430.

14. Breecker D, Sharp ZD, McFadden L (2009) Seasonal bias in the formation and stable isotope composition of pedogenic carbonate in modern soils from central New Mexico, USA. *Geol Soc Am Bull*, 121:630–640.
15. Cerling TE (1984) The stable isotopic composition of modern soil carbonate and its relationship to climate. *Earth Planet Sc Lett*, 71:229–240.
16. Cerling TE (1999) *Palaeoweathering, palaeosurfaces and related continental deposits. Special Publication of the International Association of Sedimentologists*, ed Simon-Coincon R (Blackwell, Cambridge), pp 43–60.
17. Romanek CS, Grossman EL, Morse JW (1992) Carbon isotopic fractionation in synthetic aragonite and calcite—Effect of temperature and precipitation rate. *Geochim Cosmochim Acta*, 56:419–430.
18. Brook GA, Folkoff ME, Box EO (1983) A world model of soil carbon dioxide. *Earth Surf Proc Land*, 8:79–88.
19. Mielnick PC, Dugas WA (2000) Soil CO_2 flux in a tallgrass prairie. *Soil Biol Biochem*, 32:221–228.
20. Norman JM, Garcia R, Verma SB (1992) Soil surface CO_2 fluxes and the carbon budget of a grassland. *J Geophys Res*, 97:18 845–18 853.
21. Harper CW, Blair JM, Fay PA, Knapp AK, Carlisle JD (2005) Increased rainfall variability and reduced rainfall amount decreases soil CO_2 flux in a grassland ecosystem. *Glob Change Biol*, 11:322–334.
22. Franzluebbers K, Franzluebbers AJ, Jawson MD (2002) Environmental controls on soil and whole-ecosystem respiration from a tallgrass prairie. *Soil Sci Soc Am J*, 66:254–262.
23. Liu X, Wan S, Su B, Hui D, Luo Y (2002) Response of soil CO_2 efflux to water manipulation in a tallgrass prairie ecosystem. *Plant Soil*, 240:213–223.
24. Gupta SR, Singh JS (1981) Soil respiration in a tropical grassland. *Soil Biol Biochem*, 13:261–268.
25. Pinto AS, et al. (2002) Soil emissions of N_2O, NO and CO_2 in Brazilian Savannas: Effects of vegetation type, seasonality and prescribed fires. *J Geophys Res*, 107:8089–8097 doi:10.1029/2001JD000342.
26. Medina E, Klinge H, Jordan C, Herrera R (1980) Soil respiration in Amazonian rain forests in the Rio Negro Basin. *Flora*, 170:240–250.
27. Werner C, et al. (2006) N_2O, CH_4 and CO_2 emissions from seasonal tropical rainforests and a rubber plantation in Southwest China. *Plant Soil*, 289:335–353.
28. Wood WW, Petraitis MJ (1984) Origin and distribution of carbon dioxide in the unsaturated zone of the southern high plains of Texas. *Water Resour Res*, 20:1193–1208.
29. Parada CB, Long A, Davis SN (1983) Stable isotopic composition of soil carbon dioxide in the Tucson Basin, Arizona, USA. *Chem Geol*, 1:219–236.
30. Amundson R, Chadwick OA, Sowers JM (1989) A comparison of soil climate and biological activity along an elevation gradient in the eastern Mojave Desert. *Oecologia*, 80:395–400.
31. de Jong E (1981) Soil aeration as affected by slope position and vegetative cover. *Soil Sci*, 131:34–43.
32. Indermühle A, et al. (1999) Holocene carbon-cycle dynamics based on CO_2 trapped in ice at Taylor Dome, Antarctica. *Nature*, 398:121–126.
33. Retallack G (2009) Refining a pedogenic-carbonate CO_2 paleobarometer to quantify a middle Miocene greenhouse spike. *Palaeogeogr Palaeocl*, 281:57–65.
34. McFadden LD, Tinsley JC (1985) *Soils and Quaternary geology of the southwest United States Geological Society of America Special Paper 203*, ed Weide DL (Geological Society of America, Boulder), pp 23–41.
35. Demicco RV, Lowenstein TK, Hardie LA (2003) Atmospheric pCO_2 since 60 Ma from records of seawater pH, calcium, and primary carbonate mineraology. *Geology*, 31:793–796.
36. Pagani M, Zachos JC, Freeman KH, Tipple B, Bohaty S (2005) Marked decline in atmospheric carbon dioxide concentrations during the Paleogene. *Science*, 309:600–603.
37. Beerling DJ, McElwain JC, Osborne CP (1998) Stomatal responses of the 'living fossil' Ginkgo biloba L. to changes in atmospheric CO_2 concentrations. *J Exp Bot*, 49:1603–1607.
38. Berner RA (2008) Addendum to "Inclusion of the weathering of volcanic rocks in the GEOCARBSULF model". *Am J Sci*, 308:100–103.
39. Chen L.-Q, et al. (2001) Assessing the potential for the stomatal characters of extant and fossil Ginkgo leaves to signal atmospheric CO_2 change. *Am J Bot*, 88:1309–1315.
40. Cleveland DM, Nordt LC, Dworkin SI, Atchley SC (2008) Pedogenic carbonate isotopes as evidence for extreme climatic events preceding the Triassic-Jurassic boundary: Implications for the biotic crisis?. *Geol Soc Am Bull*, 120:1408–1415.
41. Feng W, Yapp CJ (2009) Paleoenvironmental implications of concentration and $^{13}C/^{12}C$ ratios of $Fe(CO_3)OH$ in goethite from a mid-latitude Cenomanian laterite in southwestern Minnesota. *Geochim Cosmochim Acta*, 73:2559–2580.
42. Kürschner WM, Kvacek Z, Dilcher DL (2008) The impact of Miocene atmospheric carbon dioxide fluctuations on climate and the evolution of terrestrial ecosystems. *Proc Natl Acad Sci USA*, 105:449–453.
43. Lowenstein TK, Demicco RV (2006) Elevated Eocene atmospheric CO_2 and its subsequent decline. *Science*, 313:1928.
44. Passalia MG (2009) Cretaceous pCO_2 estimation from stomatal frequency analysis of gymnosperm leaves of Patagonia, Argentina. *Palaeogeogr Palaeocl*, 273:17–24.
45. Prochnow SJ, Nordt LC, Atchley SC, Hudec MR (2006) Multi-proxy paleosol evidence for middle and late Triassic climate trends in eastern Utah. *Palaeogeogr Palaeocl*, 232:53–72.
46. Quan C, Sun C, Sun Y, Sun G (2009) High resolution estimates of paleo-CO_2 levels through the Campanian (Late Cretaceous) based on Ginkgo cuticles. *Cretaceous Res*, 30:424–428.
47. Retallack GJ (2009) Greenhouse crises of the past 300 million years. *Geol Soc Am Bull*, 121:1441–1455.
48. Sun B, et al. (2007) Quantitative analysis of paleoatmospheric CO_2 level based on stomatal characters of fossil Ginkgo from Jurassic to Cretaceous in China. *Acta Geologica Sinica*, 81:931–939.
49. Crowley TJ (1998) *Tectonic Boundary Conditions for Climate Reconstructions*, ed Crowley TJ (Oxford Univ Press, New York), pp 3–17.